Navigability of interconnected networks under random failures

Manlio De Domenico, Albert Solé-Ribalta, Sergio Gómez, and Alex Arenas[1]

Departament d'Enginyeria Informàtica i Matemàtiques, Universitat Rovira i Virgili, 43007 Tarragona, Spain

Edited* by H. Eugene Stanley, Boston University, Boston, MA, and approved April 28, 2014 (received for review September 30, 2013)

Assessing the navigability of interconnected networks (transporting information, people, or goods) under eventual random failures is of utmost importance to design and protect critical infrastructures. Random walks are a good proxy to determine this navigability, specifically the coverage time of random walks, which is a measure of the dynamical functionality of the network. Here, we introduce the theoretical tools required to describe random walks in interconnected networks accounting for structure and dynamics inherent to real systems. We develop an analytical approach for the covering time of random walks in interconnected networks and compare it with extensive Monte Carlo simulations. Generally speaking, interconnected networks are more resilient to random failures than their individual layers per se, and we are able to quantify this effect. As an application—which we illustrate by considering the public transport of London—we show how the efficiency in exploring the multiplex critically depends on layers' topology, interconnection strengths, and walk strategy. Our findings are corroborated by data-driven simulations, where the empirical distribution of check-ins and check-outs is considered and passengers travel along fastest paths in a network affected by real disruptions. These findings are fundamental for further development of searching and navigability strategies in real interconnected systems.

Network theory has been revealed to be a perfect instrument to model the structure of complex systems and the dynamical process in which they are involved. However, the classical approach does not take into account the possibility that agents can be networked in different ways, and with different intensity, on multiple layers simultaneously. As an example, in the case of social sciences the same user might choose to subscribe to two or more online social networks and to build different social relationships with different users on each social platform (e.g., LinkedIn for the network of professional contacts, Facebook for the network of friends, etc.). Another example is represented by transportation networks in a city: the network of bus stops, the first layer, is different from the tube network, the second layer, but people make use of both by combining paths to move from one place to another within the city. The cases where one vertex is not present in the full multiplex can be accounted for by including it as an isolated vertex in the layers where it is missing, without altering either topological or dynamical properties of the interconnected network.

The existence of such multiple connections on different layers invites a generalization of the theory of complex networks to cope with multilayer interconnected networked systems. More specifically, very recent studies focused on a particular type of multilayer network, the multiplex, where each agent participates in different layers simultaneously, like our previous example in the case of online social networks. Indeed, the actors (vertices) in every layer are the same and are indeed vectors of multiplex states that can self-interact, at variance with interdependent networks which are conceived as interconnected communities within a single, larger network (1, 2).

The emergent physics of dynamical processes on top of multiplex networks has still to be discovered and formalized. Recently, it has been shown that diffusion processes in multiplex can have an enhanced-diffusive behavior (3), meaning that the time scales associated with diffusion in the whole multiplex can be shorter than those associated with the individual layers. This phenomenon is strictly related to the particular setup of the multiplex, and has no counterpart in classical "monoplex" networks.

Moreover, it has been recently shown that any real-world interconnected system is potentially at risk for abrupt changes in its structure, which may manifest new dynamical properties (4). However, diffusion processes describe states of vertices in terms of continuous variables that can be differentiated, whereas real diffusive processes in networks are better represented by a finite number of discrete visits (e.g., communication in online social networks, people commuting in transportation networks, etc.). A natural way to represent these processes in physics, and in particular in networks, is by considering random walkers (5–10), whose exploration of the full networked system is akin to a diffusion process (11) and might help, for instance, to uncover community structures on multiple layers (12), to infer gene regulatory pathways (13), to identify genes associated with hereditary disorders in protein–protein interaction networks (14), or to model first-passage time in complex disordered media (15).

The implications of the study of random walks, however, go beyond the scope of physics, and are useful in other disciplines such as financial time series analysis (16), genetics (17, 18), evolution (19), social sciences (20), contagion processes (21–23), and to rank websites in the world wide web by importance and quality (24), to cite a few.

Here we focus on this specific type of dynamical process on interconnected networks, i.e., random walks. We estimate analytically the coverage of multilayer interconnected networks for several types of random walks. This estimation allows us to quantify the differences in navigability, and its resilience to

Significance

Network theory has been exploited in the last decades to deepen our comprehension of complex systems. However, real-world complex systems exhibit multiple levels of relationships and require modeling by interconnected networks, characterizing interactions on several levels simultaneously. Questions such as "what is the efficiency of exploration of a city using the multiple transportation layers, like subway and bus?" and "what is its resilience to failures?" have to be answered using the multiplex framework. Here, we introduce fundamental mechanisms to perform such exploration, using random walks on multilayer networks, and we show how the topological structure, together with the navigation strategy, influences the efficiency in exploring the whole structure.

Author contributions: M.D.D., A.S.-R., S.G., and A.A. designed research, performed research, contributed new reagents/analytic tools, analyzed data, and wrote the paper.

The authors declare no conflict of interest.

*This Direct Submission article had a prearranged editor.

[1]To whom correspondence should be addressed. E-mail: alexandre.arenas@urv.cat.

This article contains supporting information online at www.pnas.org/lookup/suppl/doi:10.1073/pnas.1318469111/-/DCSupplemental.

random failures, of multilayer networks with respect to the navigability of the individual layers.

At variance with other navigation problems in science and technology, only local information of network is required, i.e., any source vertex does not possess the knowledge of the entire topology. It has been shown that the design and development of optimal navigation can be achieved exploiting shortest paths, either with local knowledge and the presence of long-range connections in a lattice network (25) or by imposing cost constraints, regardless of the available (global or local) information (26). However, in the presence of random failures it is not possible to have real-time information about the subsequent congestion. Moreover, the catastrophic cascade of failures, which might follow because of the interdependence of transport systems (27), is likely to propagate along shortest paths affecting the vertices with highest betweenness (28). Random walks represent a good choice to overcome this problem, and a good proxy to the real scenario. The coverage of random walks is a rich concept of interest in many phenomena, from ecology to physics (29, 30), as it provides a quantitative measure of the territory explored by a diffusing particle. For instance, its generalization to the number of distinct sites visited by several agents randomly walking simultaneously allowed a range of important problems to be solved, as in mathematical ecology (31).

We illustrate an application to the real-world problem of traveling efficiently in a transportation network. In particular, we consider the public transport of London, where each layer corresponds to a different type of rail network, and we show how neglecting to account for the cost of switching between layers of a multiplex can lead to an underestimation or an overestimation of navigability and exploration performances, as well as to its resilience. We corroborate our findings by performing data-driven simulations, considering the empirical distribution of check-ins and check-outs in the transportation system and assuming passengers traveling along fastest paths connecting two stations. Moreover, we simulate real disruptions, according to "no service" status reported by the Transport for London system. We show that the resilience of the whole interconnected structure under random failures, quantified by assuming a random-walk strategy, successfully captures the resilience calculated using empirical data and fastest-path strategies, providing a good approximation to the real resilience. The overall results show quantifiable dependences between the dynamical process and the underlying topology that are of utmost importance in the design of searching–routing–exploring strategies in real interconnected networks.

Results

Modeling Multilayer Relationships of Networked Systems. A multiplex network is a multilayer graph where vertices belong to several different layers (i.e., monoplex networks) simultaneously, and they are connected by means of a specific set of edges in each layer. The weighted intralayer connection between two vertices i and j in the layer α of the multiplex is indicated by $W_{ij}^{(\alpha)}$, where we use Latin letters to indicate vertices $(i,j=1,2,\ldots,N)$ and Greek letters for indices indicating layers $(\alpha=1,2,\ldots,L)$.

Because of the peculiar interconnected structure, it is possible to move from one layer to another one, provided that such layers are connected with each other. We show in Fig. 1 a representative example of a multiplex topology, where each layer is connected bidirectionally to the other layers. The interlayer connections among the layers present in the multiplex define a networked system at a macroscopic level. To account for this network of layers, representing a fundamental characteristic of the multiplex, we introduce here the matrix $D_{(i)}^{\alpha\beta}$ to quantify the cost to switch from layer α to layer β for a walker placed in a vertex i.

Therefore, it is useful to distinguish between the strength $s_{i,\alpha}=\sum_j W_{ij}^{(\alpha)}$ of a vertex i with respect to its connections with other vertices j $(j=1,2,\ldots,N)$ in the same layer α, and the strength $S_{i,\alpha}=\sum_\beta D_{(i)}^{\alpha\beta}$ of the same vertex with respect to connections to its counterparts in different layers. For the sake of simplicity, in the following we consider that the cost to switch between any pair of layers is $D_{(i)}^{\alpha\beta}=D_X$ for all vertices.

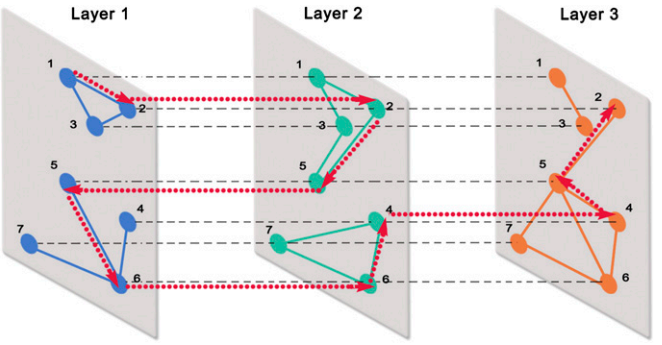

Fig. 1. Example of the navigation on an interconnected network. Path (dotted red line) of a random walker exploiting the multiplex topology to find a way around to jump between disconnected components. In this example the walker is not allowed to switch between layer 1 and layer 3 in one time step.

Navigation on an Interconnected Network. At a microscopic level, we can reduce the problem of describing the walk dynamics between vertices and layers per time unit to the definition of four fundamental transition rules accounting for all possibilities. In fact, we have (i) $\mathcal{P}_{ii}^{\alpha\alpha}$, the probability of staying for one time step in the same vertex i and in the same layer α; (ii) $\mathcal{P}_{ij}^{\alpha\alpha}$, the probability of staying in the same layer α while moving from vertex i to a vertex $j\neq i$ in its neighborhood; (iii) $\mathcal{P}_{ii}^{\alpha\beta}$, the probability of staying in the same vertex while switching to its counterpart from layer α to layer $\beta\neq\alpha$; (iv) $\mathcal{P}_{ij}^{\alpha\beta}$, the probability of moving from vertex i to vertex $j\neq i$ while switching from layer α to layer $\beta\neq\alpha$, in the same time step. Within such prescriptions, the master equation describing the probability of finding the walker in vertex j and in layer β at time $t+\Delta t$ is given by

$$p_{j,\beta}(t+\Delta t)=\mathcal{P}_{jj}^{\beta\beta}p_{j,\beta}(t)+\sum_{\substack{\alpha=1\\ \alpha\neq\beta}}^{L}\mathcal{P}_{jj}^{\alpha\beta}p_{j,\alpha}(t)+\sum_{\substack{i=1\\ i\neq j}}^{N}\mathcal{P}_{ij}^{\beta\beta}p_{i,\beta}(t)+\sum_{\substack{\alpha=1\\ \alpha\neq\beta}}^{L}\sum_{\substack{i=1\\ i\neq j}}^{N}\mathcal{P}_{ij}^{\alpha\beta}p_{i,\alpha}(t), \quad [1]$$

where the terms account for transitions (i)–(iv) described above. We indicate with $\mathbf{p}_\alpha$ the row vector with N components $p_{i,\alpha}$ with respect to layer α, and we introduce the supravector $\mathbf{P}\equiv(\mathbf{p}_1,\mathbf{p}_2,\ldots,\mathbf{p}_L)$ with NL components. Moreover, in the special case with $\Delta t=1$ we have $\dot{\mathbf{P}}(t)=\mathbf{P}(t+1)-\mathbf{P}(t)$. Therefore, Eq. **1** can be written in a more compact form as $\dot{\mathbf{P}}(t)=-\mathbf{P}(t)\mathcal{L}$, hereafter referred to as the random-walker equation. In this equation, $\mathcal{L}$ is the $NL\times NL$ normalized supra-Laplacian matrix, whose structure is similar, although not identical, to the supra-Laplacian matrix recently proposed in ref. 3 to model the diffusion process in a multiplex network (*SI Appendix*).

The structure of the random-walk equation is the same regardless of the transition rules adopted to describe any particular case of interest. See *SI Appendix* for further details about the navigation strategies considered in this study, the transition rules, and the occupation probability.

Exploration Efficiency of an Interconnected Network. In the following we will consider only multiplex networks with undirected

intra- and interlayer connections. To quantify the efficiency of the random walk in exploring the multiplex network, we focus on the coverage $\rho(t)$, defined as the average fraction of distinct vertices visited at least once in a time less than or equal to t, regardless of the layer, assuming that walks started from any other vertex in the network. We find that a good approximation to the coverage (*Materials and Methods*) is given by

$$\rho(t) = 1 - \frac{1}{N^2}\sum_{i,j=1}^{N} \delta_{ij}(0)\exp\left[-\mathbf{P}_j(0)\mathbb{P}\mathbf{E}_i^{\dagger}\right], \qquad [2]$$

where $\mathbf{P}_j(0)$ indicates the supravector of probabilities at time $t=0$ (assuming that the walker started in vertex j), the matrix $\mathbb{P}$ accounts for the probability to reach each vertex through any path of length $1, 2, \ldots$ or $t+1$, and $\mathbf{E}_i^{\dagger}$ is a supracanonical vector allowing one to compact the notation. Eq. **2** can be solved numerically to obtain the correct coverage at each time step. It is worth noting that Eq. **2** shows how the exploration of a multiplex network is influenced by different factors encoded in the matrix $\mathbb{P}$, i.e., the topological structure of each layer, the strength of interlayer connections, and the exploration strategy defined by random-walk transition rules. All these factors critically determine the time scale to cover the network. From the eigendecomposition of the supra-Laplacian, the alternative representation

$$\rho(t) \approx 1 - \frac{1}{N^2}\sum_{i,j=1}^{N} \Delta_{ij} e^{-\mathcal{C}_{i,j}(1)t - \mathcal{C}_{i,j}(2)\lambda_2^{-1}}, \qquad [3]$$

can be obtained (*Materials and Methods*). To validate our theoretical predictions, we consider different two-layer multiplex topologies, where each layer can be a Barabási–Albert (BA) network (32), an Erdős–Rényi (33) or a Watt–Strogatz graph (34). For each multiplex topology random-walk rules and interlayer weights are fixed, and from each vertex we simulate the propagation of 100 random walkers for 10^4 time steps. Therefore, we estimate the average fraction of visited vertices from the random-walk ensemble as a function of time. In Fig. 2 we show the comparison between the coverage obtained from detailed Monte Carlo simulations and the predictions given by Eqs. **2** and **3**, for three different interconnected topologies. The theoretical curves approximate the simulations quite well, with small differences only for the case of BA + BA topology, the multiplex with highest heterogeneity among the shown scenarios. In *SI Appendix* we show additional representative examples demonstrating that the multiplex topology and the navigation strategy have an evident impact on the walk process, delaying or accelerating the exploration of the network with respect to

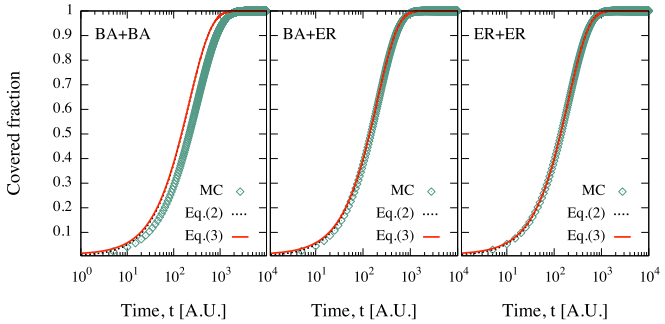

Fig. 2. Theoretical description of the navigability of a multiplex against simulation. Coverage versus time obtained from Monte Carlo simulations and our theoretical predictions given by Eqs. **2** and **3**. A two-layer multiplex with $D_X = D^{11} = D^{22} = 1$ is considered.

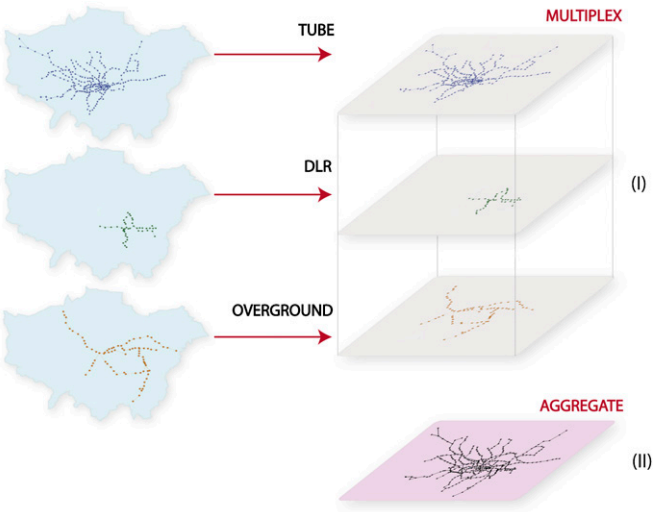

Fig. 3. Multilayer network of public transport of London. (*I*) Tube, overground, and DLR define three layers of the multiplex transportation network. Each station, individuated by a geographical position, represents a vertex, whereas the existence of a real connection between two stations defines the presence of an edge. (*II*) Aggregate network corresponding to the weighted projection of the multiplex to a single-layer graph, where the information about the type of transport is lost.

a navigation in a monoplex random network. This is a genuine effect of the multilayer structure whose control might help to build multilayer structures or strategies enhancing or reducing the navigability of the network.

Application to the Public Transport of London. The study of the navigability performance on cities is a large area of study; see, for instance, refs. 35 and 36 and references therein. In particular, a recent study (37) presents a remarkable analysis of the path optimization processes behind the transportation facilities in a large city like London. In fact, with more than 10 million inhabitants, London requires an efficient transportation network allowing people to move easily and quickly through the city. Here, we assume a more abstract scenario to get insight about the fundamental interrelations between the dynamical process and the underlying topology of the transportation network in London. We consider three different layers of such a network, namely the tube, the overground, and the docklands light railway (see *Materials and Methods* for further detail about the dataset). Each station represents a vertex, whereas real connections between stations are considered as weighted links (see Fig. 3*I* for a schematic illustration). We also show the corresponding aggregate network, obtained by the weighted projection of the multiplex to a single-layer graph, where the information about the type of transport is lost (Fig. 3*II*). Only a few stations exist simultaneously on more than one transportation layer.

We capitalize on the presented theoretical framework to investigate the navigability resilience of interconnected networks to random failures, focusing on the particular case of the public transport of London. A failure here is considered as the inoperability of a station in a certain transportation layer (e.g., because of an accident, a traffic jam, or catastrophe). Such an event can happen randomly on the system and can affect one or more stations at the same time. A measure of the operability of the full system in response to unexpected failures can be inferred from the coverage of the respective networks after such events. This is what we call the navigability resilience. The resilience $r(\phi)$ of the system to a fraction ϕ of random failures is defined by $r(\phi) = \langle \rho_\phi(\tau) \rangle / \rho_0(\tau)$, where $\rho_\phi(t)$ is the coverage at time t of the network

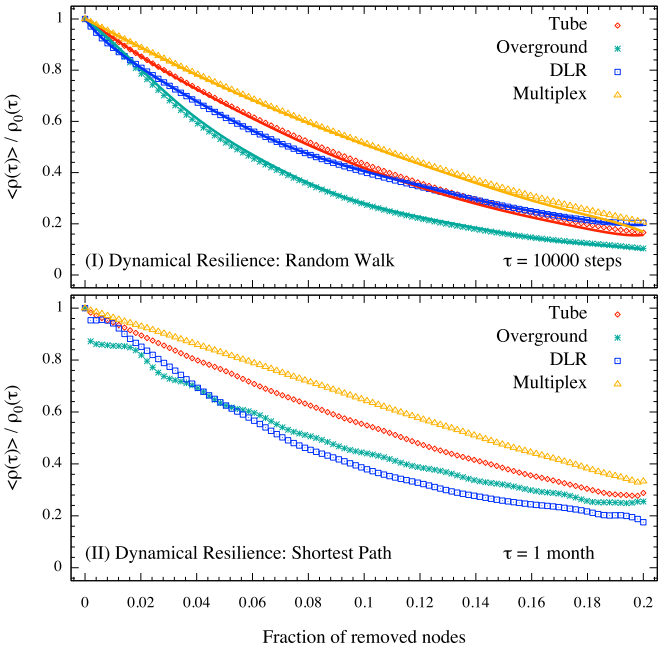

Fig. 4. Resilience of the public transport network of London to random failures. (*I*) Theoretical expectations (solid lines) reproduce with great accuracy the resilience (points) obtained from simulations for each transportation layer and the whole interconnected system ($D_X = 10^{-1}$), assuming random-walk-based navigation. (*II*) The same as *I* but assuming shortest-path-based navigation and empirical data.

subjected to ϕ failures and the averages are calculated over several random realizations of the failures. The normalization guarantees a fair comparison between the resilience of the multiplex and the monoplex networks. When a vertex fails in a single transportation layer, it cannot be traversed by any path. However, if that vertex is part of an interconnected network it can still be reached on other layers. This intrinsic feature of multiplexes enhances the resilience of the system with respect to monoplexes, as shown in Fig. 4, *I* for the public transport of London. Eqs. **2** and **3** are used to predict the resilience obtained by extensive simulations, and results are reproduced with great accuracy.

To evaluate the resilience of the system in a more realistic scenario, we consider the empirical distribution of check-ins and check-outs in the public transport of London and we simulate passengers traveling along the shortest paths connecting two stations. We consider the adjacency matrices of each transportation system and we construct a weighted interconnected network where weights represent the cost to move between two connected stations. Here, the cost corresponds to the time required by an individual to travel along a connection, assuming that the involved modes of transport travel with an average speed of 33 km/h (38). Because the commutation time is not available, we assume it corresponds, on average, to the time an individual requires to walk 500 m with an average speed of 5 km/h. For each "shortest-path" walker, the starting and ending stations are sampled according to the data. When a destination is reached we consider it as a new starting station and a new target is sampled, iterating this procedure for 1 mo. As for the random-walk strategy, the coverage is given by the fraction of stations visited over time. In the case of random failures, the cost matrix is recalculated "on the fly" to simulate the behavior of individuals more realistically. We show in Fig. 4, *II* the resilience obtained in this case, in agreement with the estimation obtained assuming random-walk-based strategies. Our results show that resilience based on random-walk navigation provides an approximation to the empirical one.

For the sake of completeness, see *SI Appendix* for the topological resilience corresponding to the same multiplex, defined by the average fraction of vertices surviving in the giant connected component after random failures. The navigability, i.e., the dynamical resilience, is inherently smaller than the topological resilience of this multiplex network.

We also report the numerical resilience, and its theoretical expectation, in the case of real disruptions affecting the transportation network of London (Table 1 and *SI Appendix*). Our predictions are in excellent agreement with numerical simulations and, in the case of more realistic simulation, they always provide a good approximation of empirical resilience.

Discussion

Our world is inherently networked and actors coexist in several different levels of relationships. People interacting during financial transactions and in real (or virtual) social systems, goods moving from one location to another by means of different modes of transport (e.g., air, rail, and road), and information flowing through different media (e.g., radio, satellite, and internet) represent important multilayer systems. Recently, progress has been made to include such levels in network analysis within the more general framework of interconnected networks (12, 39), accounting for the influence of their topologies and their interconnections to dynamical processes taking place on the networked system (3, 4). The lack of a systematic theory of random walkers on multilayer systems and their crucial role in the description of a wide variety of real-world systems, as resilience to random failures, has motivated our study. More specifically, we have investigated the behavior of different walks on interconnected networks and characterized their main statistical properties. We have identified in the coverage a suitable proxy for the exploration efficiency of the network, providing an accurate theoretical and analytical description. Our results have shown how the exploration of a multiplex is influenced by different factors. On one hand, the topological structure of each layer and the strength of interlayer connections determine the "topological reachability" of vertices, where more peripherals agents are more difficult to be visited because of their poorly influential position in the network. On the other hand, the exploration strategy

Table 1. Real disruptions in London transportation network

Line	From	To	Freq., %	Affected, %	Theory, %	RW, %	SP, %
DLR	Beckton	Canningtown	2.56	2.44	94.41	93.10	94.85
Piccadilly	Actontown	Arnosgrove	0.04	6.77	88.49	86.51	90.85
Northern	Highbarnet	Stockwell	0.08	5.96	86.11	82.55	84.49
Northern	Charingcross	Highbarnet	0.25	4.61	90.67	87.99	91.32

Representative partial line disruptions "From"–"To" stations are considered. The rate of occurrence "Freq." is reported together with the fraction of stations indirectly "Affected." The resilience obtained from Monte Carlo simulations (random walk, RW, and shortest-path, SP) are reported together with our theoretical expectation. See full table in *SI Appendix*.

defined by random-walk transition rules determine the "dynamical reachability" of vertices, where agents are more difficult to be visited because their position in the network is not privileged with respect to the flow of information. All such factors critically determine the time scale to cover the network.

To show the potential of the developed framework, we have considered an application to the public transport of London, focusing on three different transportation layers, i.e., tube, overground, and docklands light railway. We have investigated the resilience of this interconnected transport network to random failures, a study of importance to design and protect critical infrastructures. We have shown, theoretically and by means of extensive simulations, how the whole system is more resilient to random failures than its individual layers separately. Indeed, interconnected networks introduce additional dimensions that can help to find paths from apparently isolated parts of single layers, enhancing the resilience to random failures, and we provide a way to quantify this.

The results can be used to design optimal searching strategies (in the line of the findings in ref. 40), for instance, to characterize the cyclic structure of the multiplex (41), to infer gene regulatory pathways (13), to coarse grain the network structure (42), to assess the PageRank in these topologies (43), or to identify genes associated with hereditary disorders in protein–protein interaction networks (14), providing a step for further development of searching and navigability strategies in real interconnected systems.

Materials and Methods

Derivation of the Coverage: Transition Matrix. To quantify the efficiency of the random walk in exploring the multiplex network, we focus on the coverage $\rho(t)$, defined as the average fraction of distinct vertices visited at least once in a time less than or equal to t, regardless of the layer, assuming that walks started from any other vertex in the network.

Let $p_i(t)=\sum_\alpha p_{i,\alpha}(t)$ be the probability to find the walker in vertex i at time t regardless of the layer. We introduce the supravector $\mathbf{E}_i\equiv(\mathbf{e}_i,\mathbf{e}_i,\ldots,\mathbf{e}_i)$, $\mathbf{e}_i$ being the ith canonical vector, to obtain $p_i(t+1)=\mathbf{P}(t)\mathcal{P}\mathbf{E}_i^\dagger$. The probability to not find the walker in vertex i after t time steps, assumed that it started in vertex j, is given by $\delta_{i,j}(t)=\coprod_{\tau=1}^{t}[1-p_i(t-\tau)][1-p_j(0)]$. Moreover, the recursive equation $\delta_i(t+1)=\delta_i(t)[1-p_i(t+1)]$ leads to

$$\dot{\delta}_{i,j}(t)=-\delta_{i,j}(t)\mathbf{P}(t)\mathcal{P}\mathbf{E}_i^\dagger. \qquad [4]$$

The solution of Eq. **4** is given by

$$\delta_{i,j}(t)=\delta_{i,j}(0)\exp\left[-\mathbf{P}_j(0)\mathbb{P}\mathbf{E}_i^\dagger\right],\quad \mathbb{P}=\sum_{\tau=0}^{t}\mathcal{P}^{\tau+1}, \qquad [5]$$

where $\mathbf{P}_j(0)\equiv(\mathbf{e}_j,\mathbf{0},\ldots,\mathbf{0})$ explicitly indicates that at time $t=0$ the walker started in vertex j and in the first layer, without loss of generality. The matrix $\mathbb{P}$ has a clear meaning: it accounts for the probability to reach each vertex through any walk of length 1,2, ... or $t+1$. Moreover, $\delta_{i,j}(0)=0$ for $j=i$ (i.e., the random walker starts in vertex i and the probability of not finding it in the same vertex must be zero) and 1 otherwise. Therefore, a good approximation to the coverage is given by double averaging over all vertices the probability $1-\delta_{i,j}(t)$, obtaining Eq. **2**, which can be solved numerically to obtain the correct coverage at each time step.

Derivation of the Coverage: Eigendecomposition. The time evolution of the supravector of probabilities $\mathbf{P}$ for a walker starting from vertex j is also given by $\mathbf{P}(t)=\mathbf{P}_j(0)e^{-\mathcal{L}t}$, $\mathcal{L}$ being the normalized supra-Laplacian matrix. From eigendecomposition of the normalized supra-Laplacian, we obtain

$$\mathbf{P}(t)=\mathbf{P}_j(0)e^{-\mathcal{L}t}=\mathbf{P}_j(0)\sum_{\ell=1}^{NL}e^{-\lambda_\ell t}\mathcal{V}_\ell, \qquad [6]$$

where each supramatrix $\mathcal{V}_\ell$ is obtained from products of eigenvectors. By substituting this expression into Eq. **4** for the dynamical evolution of $\delta_{i,j}(t)$, we obtain

$$\frac{\dot{\delta}_{i,j}(t)}{\delta_{i,j}(t)}=-\sum_{\ell=1}^{NL}e^{-\lambda_\ell t}\mathcal{C}_{i,j}(\ell), \qquad [7]$$

where $\mathcal{C}_{i,j}(\ell)=\mathbf{P}_j(0)\mathcal{V}_\ell\mathcal{P}\mathbf{E}_i^\dagger$ are constants depending on the vertex, the transition matrix, the eigendecomposition, and the initial conditions. Let us recall that the coverage is defined by double averaging the probability $1-\delta_{i,j}(t)$ over all vertices. Hence, another expression for the coverage versus time, alternative to Eq. **2**, is given by

$$\rho(t)=1-\frac{1}{N^2}\sum_{i,j=1}^{N}\delta_{i,j}(0)\exp\left[-\mathcal{C}_{i,j}(1)t-\sum_{\ell=2}^{NL}\mathcal{C}_{i,j}(\ell)\frac{e^{-\lambda_\ell t}-1}{-\lambda_\ell}\right].$$

After enough time, i.e., $\lambda_2 t\gg 1$, the sum in the above exponentials is dominated by the term with $\ell=2$ and, additionally, $e^{-\lambda_2 t}\ll 1$, leading to Eq. **3**. Note that for normalized supra-Laplacian matrices with more than one null eigenvalue, the more general version of Eq. **3** is given by

$$\rho(t)=1-\frac{1}{N^2}\sum_{i,j=1}^{N}\delta_{i,j}(0)\exp\left[-\sum_{\ell\in\Lambda^0}\mathcal{C}_{i,j}(\ell)t-\sum_{\ell\in\Lambda^+}\mathcal{C}_{i,j}(\ell)\frac{e^{-\lambda_\ell t}-1}{-\lambda_\ell}\right],$$

where Λ^0 and Λ^+ indicate the sets of all null and positive eigenvalues of the normalized supra-Laplacian, respectively.

Overview of the Dataset. The list of tube, overground, and docklands light railway (DLR) stations, their positions, and their coordinates have been obtained from publicly available information in the official website dedicated to the transport of London (44) and in Wikipedia (www.wikipedia.org). The total number of stations is 369, among which there are 271 vertices with 312 connections considering all lines of the tube, 83 vertices with 83 connections in the overground, and 45 vertices with 46 connections in the DLR layer. Connections are undirected and weighted, where, in the case of the tube, the weight is given by the number of different underground lines connecting two stations. Check-ins and check-outs have been obtained from a 5% sample of all Oyster card journeys performed in a week during November 2009 on bus, tube, DLR, and London overground, available from ref. 44. The empirical distributions adopted in our simulations refer to the probability of observing a check-out in a certain station conditional to the probability that a passenger started his or her journey in another one. For details about the collection of data concerning the "no service" status in this transportation network, see *SI Appendix*.

ACKNOWLEDGMENTS. The authors acknowledge Mason A. Porter and H. Rozenfeld for valuable suggestions and useful comments. This work has been supported by Ministerio de Economía y Competitividad through Grant FIS2012-38266; European Comission FET-Proactive Projects PLEXMATH (Grant 317614) and MULTIPLEX (317532), and the Generalitat de Catalunya 2009-SGR-838. A.A. also acknowledges partial financial support from the ICREA Academia and the James S. McDonnell Foundation.

1. Gao J, Buldyrev SV, Stanley HE, Havlin S (2011) Networks formed from interdependent networks. *Nat Phys* 8:40–48.
2. Dickison M, Havlin S, Stanley HE (2012) Epidemics on interconnected networks. *Phys Rev E Stat Nonlin Soft Matter Phys* 85(6 Pt 2):066109.
3. Gómez S, et al. (2013) Diffusion dynamics on multiplex networks. *Phys Rev Lett* 110(2): 028701.
4. Radicchi F, Arenas A (2013) Abrupt transition in the structural formation of interconnected networks. *Nature Physics* 9(11):717–720.
5. Stanley HE, Kang K, Redner S, Blumberg RL (1983) Novel superuniversal behavior of a random-walk model. *Phys Rev Lett* 51:1223–1226.
6. Noh JD, Rieger H (2004) Random walks on complex networks. *Phys Rev Lett* 92(11):118701.
7. Yang SJ (2005) Exploring complex networks by walking on them. *Phys Rev E Stat Nonlin Soft Matter Phys* 71(1 Pt 2):016107.
8. Samukhin AN, Dorogovtsev SN, Mendes JF (2008) Laplacian spectra of, and random walks on, complex networks: Are scale-free architectures really important? *Phys Rev E Stat Nonlin Soft Matter Phys* 77(3 Pt 2):036115.
9. Burda Z, Duda J, Luck JM, Waclaw B (2009) Localization of the maximal entropy random walk. *Phys Rev Lett* 102(16):160602.
10. Sinatra R, Gómez-Gardeñes J, Lambiotte R, Nicosia V, Latora V (2011) Maximal-entropy random walks in complex networks with limited information. *Phys Rev E Stat Nonlin Soft Matter Phys* 83(3 Pt 1):030103.
11. Costa LdaF, Travieso G (2007) Exploring complex networks through random walks. *Phys Rev E Stat Nonlin Soft Matter Phys* 75(1 Pt 2):016102.
12. Mucha PJ, Richardson T, Macon K, Porter MA, Onnela JP (2010) Community structure in time-dependent, multiscale, and multiplex networks. *Science* 328(5980): 876–878.

13. Tu Z, Wang L, Arbeitman MN, Chen T, Sun F (2006) An integrative approach for causal gene identification and gene regulatory pathway inference. *Bioinformatics* 22(14):e489–e496.
14. Köhler S, Bauer S, Horn D, Robinson PN (2008) Walking the interactome for prioritization of candidate disease genes. *Am J Hum Genet* 82(4):949–958.
15. Condamin S, Bénichou O, Tejedor V, Voituriez R, Klafter J (2007) First-passage times in complex scale-invariant media. *Nature* 450(7166):77–80.
16. Stanley HE, et al. (2002) Self-organized complexity in economics and finance. *Proc Natl Acad Sci USA* 99(Suppl 1):2561–2565.
17. Peng CK, et al. (1992) Long-range correlations in nucleotide sequences. *Nature* 356(6365):168–170.
18. Eliazar I, Koren T, Klafter J (2007) Searching circular DNA strands. *J Phys Condens Matter* 19(6):065140.
19. van Nimwegen E, Crutchfield JP, Huynen M (1999) Neutral evolution of mutational robustness. *Proc Natl Acad Sci USA* 96(17):9716–9720.
20. Newman ME (2005) A measure of betweenness centrality based on random walks. *Soc Networks* 27:39–54.
21. Daley D, Kendall DG (1965) Stochastic rumours. *J Appl Math* 1:42–55.
22. Daniels H (1967) The distribution of the total size of an epidemic. *Proceedings of the Fifth Berkeley Symposium on Mathematical Statistics and Probability* (Univ of California Press, Berkeley, CA), Vol 4, pp 281–293.
23. Maki DP, Thompson M (1973) *Mathematical Models and Applications: With Emphasis on the Social, Life, and Management Sciences* (Prentice-Hall, Englewood Cliffs, NJ).
24. Brin S, Page L (1998) The anatomy of a large-scale hypertextual web search engine. *Computer Networks and ISDN Systems* 30:107-117.
25. Kleinberg JM (2000) Navigation in a small world. *Nature* 406(6798):845.
26. Li G, et al. (2010) Towards design principles for optimal transport networks. *Phys Rev Lett* 104(1):018701.
27. Buldyrev SV, Parshani R, Paul G, Stanley HE, Havlin S (2010) Catastrophic cascade of failures in interdependent networks. *Nature* 464(7291):1025–1028.
28. Guimerà R, Díaz-Guilera A, Vega-Redondo F, Cabrales A, Arenas A (2002) Optimal network topologies for local search with congestion. *Phys Rev Lett* 89(24):248701.
29. Skellam JG (1951) Random dispersal in theoretical populations. *Biometrika* 38(1-2): 196–218.
30. Havlin S, Ben-Avraham D (1987) Diffusion in disordered media. *Adv Phys* 36:695–798.
31. Larralde H, Trunfio P, Havlin S, Stanley HE, Weiss GH (1992) Territory covered by n diffusing particles. *Nature* 355:423–426.
32. Barabási AL, Albert R (1999) Emergence of scaling in random networks. *Science* 286(5439):509–512.
33. Erdős P, Rényi A (1960) On the evolution of random graphs. *Publ Math Inst Hungar Acad Sci* 5:17–61.
34. Watts DJ, Strogatz SH (1998) Collective dynamics of 'small-world' networks. *Nature* 393(6684):440–442.
35. Helbing D (2001) Traffic and related self-driven many-particle systems. *Rev Mod Phys* 73:1067.
36. Batty M (2005) Agents, cells, and cities: New representational models for simulating multiscale urban dynamics. *Environ Plan A* 37:1373–1394.
37. Yeung CH, Saad D, Wong KY (2013) From the physics of interacting polymers to optimizing routes on the London Underground. *Proc Natl Acad Sci USA* 110(34): 13717–13722.
38. London Councils (2013) Transport for London: Key facts. Available at http://www.londoncouncils.gov.uk/londonfacts/default.htm?category=12. Accessed January 2013.
39. Szell M, Lambiotte R, Thurner S (2010) Multirelational organization of large-scale social networks in an online world. *Proc Natl Acad Sci USA* 107(31):13636–13641.
40. Viswanathan GM, et al. (1999) Optimizing the success of random searches. *Nature* 401(6756):911–914.
41. Rozenfeld HD, Kirk JE, Bollt EM, Ben-Avraham D (2005) Statistics of cycles: How loopy is your network? *J Phys A: Math Gen* 38:4589.
42. Gfeller D, De Los Rios P (2007) Spectral coarse graining of complex networks. *Phys Rev Lett* 99(3):038701.
43. Fortunato S, Boguñá M, Flammini A, Menczer F (2008) *Algorithms and Models for the Web-Graph* (Springer, Berlin Heidelberg), pp 59–71.
44. London Councils (2010) Transport for London. Available at www.tfl.gov.uk/. Accessed August 1, 2010.

Supplementary Information for "Navigability of Interconnected Networks under Random Failures"

Manlio De Domenico, Albert Solé-Ribalta , Sergio Gómez , Alex Arenas *

*Departament d'Enginyeria Informàtica i Matemàtiques, Universitat Rovira i Virgili, 43007 Tarragona, Spain

Contributed to Proceedings of the National Academy of Sciences of the United States of America

Navigation Strategies in Interconnected Networks

In the following subsection we will describe four representative random walk processes – covering a wide variety of real physical processes – and we will provide the corresponding transition rules to build the supra-Laplacian matrix, although other type of walkers, e.g., [1, 2], are also possible to implement in multiplex.

Classical random walkers. The classical description of random walkers on a graph (i.e., monoplex networks) is already present in [3, 4], although applications to networks with complex topology are more recent [5, 6].

In monoplex networks, the random walker has probability $1/k_i$ to move from vertex i to vertex j in the neighborhood of i, where k_i indicates the degree of a vertex i. The direct extension of such walks to the case of multiplex networks is to consider the inter-layer connections as additional edges available in vertex i. It follows that the probability of moving from vertex i to vertex j within the same layer α *or* to switch to the counterpart of vertex i in layer β is uniformly distributed. In such a scenario, the normalizing factor to obtain the correct probability is the total strength $s_{i,\alpha} + S_{i,\alpha}$ of vertex i. The resulting transition rules for this classical random walker in a multiplex (RWC) are given in Table 1. For sake of completeness, the Laplacian matrix corresponding to this process in monoplex networks is generally referred to as the "normalized Laplacian".

Diffusive random walkers. In monoplex networks, this type of random walk has been studied in detail in [7]. Here, at microscopic level, the random walker moves from a vertex i to one of its neighbor with hopping rate which depends on i. In fact, if $s_{\max} = \max_{i,\alpha}\{s_{i,\alpha} + S_{i,\alpha}\}$ is the maximum vertex strength in the network, the walker is allowed to wait in vertex i with rate $1 - s_i/s_{\max}$ and to jump to any vertex with rate $s_i/s_{\max}$. Hence, the nature of this walk is very different from the classical one previously described, where the hopping rate does not depend on the vertex, and it can be shown that the corresponding Laplacian matrix, once unnormalized, is equivalent to the one of the classical diffusive process (we refer to [7] for further detail).

We extend this walk to the case of multiplex networks by considering inter-layer connections as additional edges to estimate the maximum vertex strength. The resulting transition rules for this random walker in a multiplex (RWD) are given in Tab. 1.

Physical random walkers. Here we propose a new type of random walk dynamics in the multiplex, which reduces to the classical random walk in the case of monoplex. The transition rules are the same, except that we assume that the time scale to switch layer is negligible with respect to the time scale required to move from a vertex to another one in its neighborhood. Therefore, in the same time step the random walker is allowed to switch layer and to jump to another vertex, with layer-switching and the vertex-jumping actions being independent. This is a fundamental difference with the random walkers described so far, because they were not allowed to switch and jump in the same time unit. Moreover, another major difference lies in treating inter-layer connections as another type of edges, not competing with the intra-layer edges.

As an example of this dynamics, one might imagine the case of online social networks where each layer corresponds to a different social structure (e.g., Facebook and Twitter) and users play the role of vertices. In this case, the time required to a user to switch from one layer to the other one requires less than a few seconds.

The resulting transition rules for this physical random walker in a multiplex (RWP) are given in Tab. 1. It is straightforward to show that this process is equivalent to the classical random walker in the case of monoplexes.

Table 1. Transition probability for four different random walk processes on multiplex. We account for jumping between vertices (latin letters) and switching between layers (greek letters). When appearing in pairs, $j \neq i$ and $\beta \neq \alpha$ must be considered. See text for further detail.

Tr.	RWC	RWD	RWP	RWME
$\mathcal{P}_{ii}^{\alpha\alpha}$	$\frac{D_{(i)}^{\alpha\alpha}}{s_{i,\alpha}+S_{i,\alpha}}$	$\frac{s_{\max}+D_{(i)}^{\alpha\alpha}-s_{i,\alpha}-S_{i,\alpha}}{s_{\max}}$	0	$\frac{D_{(i)}^{\alpha\alpha}}{\lambda_{\max}}$
$\mathcal{P}_{ii}^{\alpha\beta}$	$\frac{D_{(i)}^{\alpha\beta}}{s_{i,\alpha}+S_{i,\alpha}}$	$\frac{D_{(i)}^{\alpha\beta}}{s_{\max}}$	0	$\frac{D_{(i)}^{\alpha\beta}}{\lambda_{\max}}\frac{\psi_{(\beta-1)N+i}}{\psi_{(\alpha-1)N+i}}$
$\mathcal{P}_{ij}^{\alpha\alpha}$	$\frac{W_{ij}^{(\alpha)}}{s_{i,\alpha}+S_{i,\alpha}}$	$\frac{W_{ij}^{(\alpha)}}{s_{\max}}$	$\frac{W_{ij}^{(\alpha)}}{s_{i,\alpha}}\frac{D_{(i)}^{\alpha\alpha}}{S_{i,\alpha}}$	$\frac{W_{ij}^{(\alpha)}}{\lambda_{\max}}\frac{\psi_{(\alpha-1)N+j}}{\psi_{(\alpha-1)N+i}}$
$\mathcal{P}_{ij}^{\alpha\beta}$	0	0	$\frac{W_{ij}^{(\beta)}}{s_{i,\beta}}\frac{D_{(i)}^{\alpha\beta}}{S_{i,\alpha}}$	0

Conflict of interest footnote placeholder

This paper was submitted directly to the PNAS office.

RWC: Classical Random Walker, RWD: Diffusive Random Walker, RWP: Physical Random Walker, RWME: Maximum Entropy Random Walker

Maximal entropy random walkers. In classical random walks, a walker jumps from a vertex to a neighbor with uniform probability which depends only on the local structure, namely the vertex strength. However, it has been recently proposed a walk dynamics where the transition rate of jumps is influenced by the global structure of the network [8], or only local information is available [2]. More specifically, the walkers choose the next vertex to jump into maximizing the entropy of their path at a global level, whereas classical random walkers maximize the entropy of their path at neighborhood level. To achieve such maximal entropy paths, the transition rates are governed by the largest eigenvalue of the adjacency matrix and the components of the corresponding eigenvector [8].

In the case of multiplex, we use the supra-adjacency matrix

$$\mathcal{A} = \left(\begin{array}{c|c|c|c} D^{11}\mathbf{I} + \mathbf{W}^{(1)} & D^{12}\mathbf{I} & \dots & D^{1L}\mathbf{I} \\ \hline D^{21}\mathbf{I} & D^{22}\mathbf{I} + \mathbf{W}^{(2)} & \dots & D^{2L}\mathbf{I} \\ \hline \vdots & & \ddots & \vdots \\ \hline D^{L1}\mathbf{I} & D^{L2}\mathbf{I} & \dots & D^{LL}\mathbf{I} + \mathbf{W}^{(L)} \end{array} \right)$$

to achieve the same result (see Materials and Methods in the main text for further detail). We indicate with $\lambda_{\max}$ the largest eigenvalue of this matrix and with ψ the corresponding eigenvector. Therefore, according to the prescription given

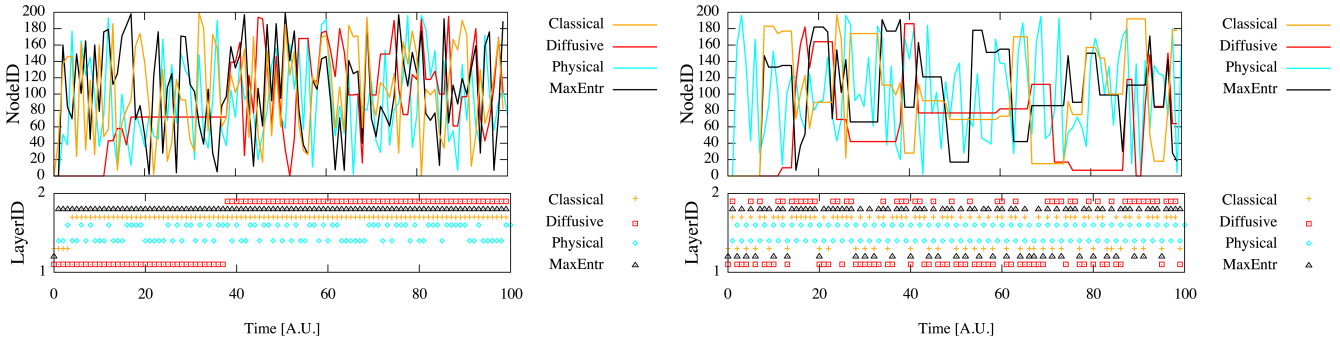

(a) BA+ER, $D^{12} = D^{21} = 1$ (b) BA+ER, $D^{12} = D^{21} = 100$

Fig. 1. Random walks realizations on different multiplex structures. Vertices (top panels) and layers (bottom panels) visited by one random walker in 100 time steps. The four types of walk considered in this study are shown. The multiplex is built with one Barabási-Albert (layer one) and one Erdős-Rényi (layer two) network with 200 vertices, while inter-layer weights are specified above.

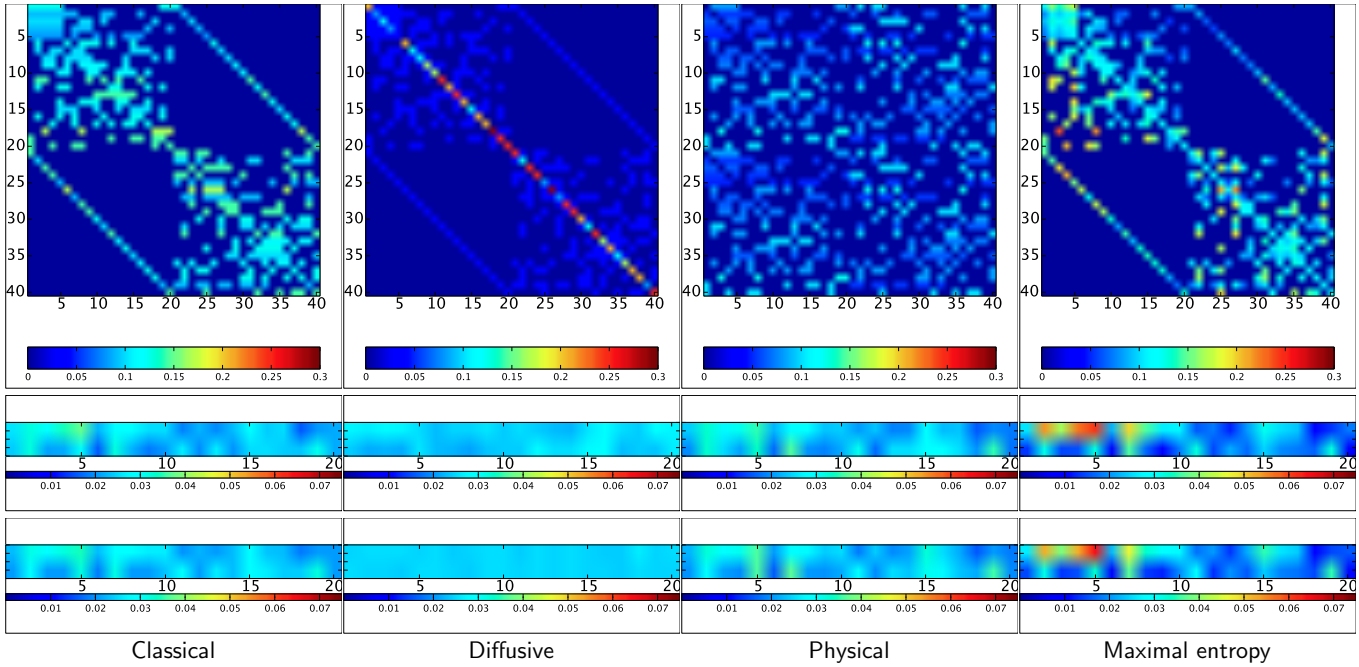

Fig. 2. Probabilities governing four random walk strategies on multiplex. *Top panels:* transition probabilities for walks considered in this study. Note that we have rescaled by a factor 2 the transition matrix of diffusive walk for better visualization and to allow comparisons. *Middle panels:* occupation probability, for each vertex in each layer, considering one random walk starting only from the first vertex. *Bottom panels:* as in middle panels, but considering one random walk starting with uniform probability from any other vertex. Multiplex of 20 vertices embedded in two different realizations of a Watts-Strogatz small-world network (rewiring probability is 0.2), where $D^{11} = D^{21} = D^{12} = D^{21} = 1$. Different exploration strategies are responsible for the different probability that a vertex is visited and occupied by a random walker.

in [8], the resulting transition rules for this maximal entropy random walker in a multiplex (RWME) are given in Tab. 1.

A representative example of each walk is shown in Fig. 1, where vertices and layers visited by one random walker up to 100 time steps are reported. We show two different cases, corresponding to different choices of inter-layer weights, to make evident the difference in the dynamics.

In the top panels of Fig. 2 we show the transition probabilities in the case of a multiplex of 20 vertices embedded in two different realizations of a Watts-Strogatz small-world network [9]. The probability to find a random walker in a certain vertex on a certain layer is also shown in the same figure, considering one walk starting from the first vertex only (middle panels) and from any other vertex with uniform probability (bottom panels). As expected, different exploration strategies result in different occupation probability, where some vertices in a certain layer might be explored more (or less) frequently, as in the case of RWC, RWP and RWME, or uniformly as in the case of RWD.

Fig. 1 and Fig. 2 clearly highlight the different dynamics and how navigation strategy influences the exploration of the multiplex.

Occupation Probability of Random Walkers

We define the *occupation probability* $\Pi_{i,\alpha} = \lim_{t\longrightarrow\infty} p_{i,\alpha}(t)$ to find a walker in vertex i of layer α in the limit $t \longrightarrow \infty$, and we indicate with $\mathbf{\Pi}$ the corresponding supra-vector. In general, $\mathbf{\Pi}$ is the left eigenvector of the supra-transition matrix corresponding to the unit eigenvalue. In some cases, the occupation probability can be estimated from the detailed balance equation

$$\Pi_{i,\alpha}\mathcal{P}_{ij}^{\alpha\beta} = \Pi_{j,\beta}\mathcal{P}_{ji}^{\beta\alpha}, \qquad [1]$$

obtaining

$$\Pi_{i,\alpha} = \frac{s_{i,\alpha} + S_{i,\alpha}}{\sum_\beta \sum_j s_{j,\beta} + S_{j,\beta}} \qquad [2]$$

for RWC, generalizing the well-known result obtained for walks in a monoplex network,

$$\Pi_{i,\alpha} = \frac{1}{NL} \qquad [3]$$

for RWD, as expected for a purely diffusive walk, and

$$\Pi_{i,\alpha} = \psi^2_{(\alpha-1)N+i}, \qquad [4]$$

for RWME, generalizing the results obtained in [8] for monoplex networks.

Indeed, following the approach proposed in [5] for random walks on monoplexes, it is possible to show that the time required to a random walker starting from vertex i to arrive back to the same vertex, i.e., the mean return time, is given by

$$\langle T_{ii}\rangle = \frac{1}{\sum_{\alpha=1}^{L} \Pi_{i,\alpha}}. \qquad [5]$$

It is straightforward to verify that distributions expected in the case of monoplex are recovered for $L = 1$. It is worth noting that for classical random walks the occupation probability of vertex i is proportional to its *supra-strength*, i.e., intra- plus inter-layer strengths, whereas for diffusive walks such a probability is the same for any vertex, regardless of multiplex topology.

Dynamical vs Topological Descriptors

We show in Fig. 3 the coverage *versus* time in the case of RWP only, for some representative multiplexes where $D^{12}_{(i)} = D^{21}_{(i)} = D^{11}_{(i)} = D^{22}_{(i)} = 1$, $\forall i = 1, 2, ..., N$. Results for different combination of topologies (double acronym in the legend) are shown, together with results for walks in a single layer (single acronym in the legend). "Diff" indicates same topology but different random realizations, while "same" indicates same topology and same random realization on both layers. Inset shows the relative difference of coverages with respect to the case of an ER monoplex.

The multiplex topology has an evident impact on the walk process, delaying or accelerating the exploration of the network with respect to a random search in a monoplex random

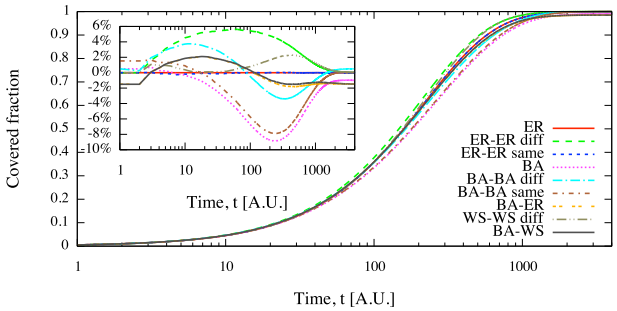

Fig. 3. Dependence of the coverage on multiplex topology. Number of visited vertices *versus* time for monoplex and multiplex topologies (see the text for further details about the simulations). The inset shows the relative difference of each curve with respect to the coverage obtained for an ER monoplex, evidencing that vertices in different topologies are visited with different time scales.

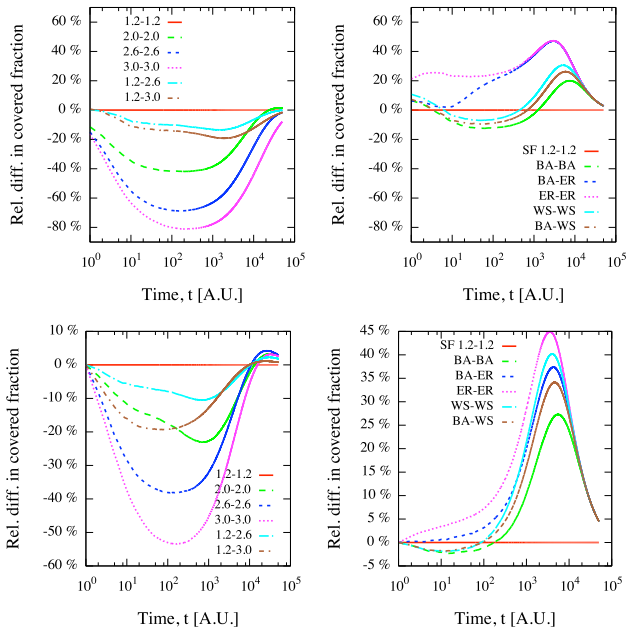

Fig. 4. Dependence of the coverage on multiplex topology. Same as the inset of Fig. 4, where the relative difference of each curve is calculated with respect to the coverage obtained for a multiplex of two different scale-free networks with degree distribution $\propto k^{-1.2}$. Top panels refer to RWC, whereas bottom panels refer to RWP. Left panels (top and bottom) refer to multiplexes of different scale-free networks with other degree distributions, whose indices are specified in the legend. Right panels (top and bottom) refer to multiplexes of other topologies.

network.

This is a genuine effect of the multi-layer structure and it is not related to the finite size of the considered networks as shown in Fig. 4, where multiplexes of 2000 nodes and many different topologies are considered.

In Fig. 5, for each random walk considered, we show the inverse of the time τ_C required to cover the 50% of a BA+ER multiplex with 200 vertices as a function of the inter-layer weight $D_X = D^{12} = D^{21}$. It is worth mentioning that the final result depends only quantitatively, but not qualitatively, on the choice of the covered fraction. This representative example shows the impact of transition rules on the exploration of the multiplex, putting in evidence that the best strategy to adopt to cover the network depends on the topology and on the weight of inter-layer connections. Moreover, in this specific experiment, the walk in the multiplex is *infra-diffusive* (*sub-diffusive*) depending on the value of D_X, i.e., the time to cover the multiplex lies between (is smaller than) the times required to cover each layer separately. It is worth noting that in other cases, like RWME on BA+BA multiplexes, walks show *enhanced diffusion*, i.e., the time to cover the multiplex is smaller than the time to cover each layer separately. This is shown, for instance, in Fig. 6.

Intriguingly, we observe a similar behavior for λ_2, i.e., the second smallest eigenvalue of the supra-Laplacian. We show in Fig. 7 the values of $1/\tau_C$ (top panels) and λ_2 (bottom panels) versus D_X for the four random walks and three different multiplex topologies with 200 vertices, namely BA+BA (left panels), BA+ER (middle panels) and ER+ER (right panels). Except for the smallest values of D_X, the behavior is the same, especially in the limit of $D_X \longrightarrow \infty$.

See the main text and the corresponding Materials and Methods for a qualitative explanation of this result. From

$$\rho(t) \approx 1 - \frac{1}{N^2} \sum_{i,j=1}^{N} \Delta_{ij} e^{-\mathcal{C}_{i,j}(1)t - \mathcal{C}_{i,j}(2)\lambda_2^{-1}}, \qquad [6]$$

the importance of λ_2 in the evolution of the coverage is evident. Let $\tau^\star$ be the time required to cover a certain fraction $\rho^\star = \rho(\tau^\star)$. For large values of $\tau^\star$, the weighted sum of exponentials in Eq. (6) is dominated by terms with largest temporal scale of exponential decay, i.e., by terms where the constants $\mathcal{C}_{i,j}(1)$ are the minimum ones. We indicate with

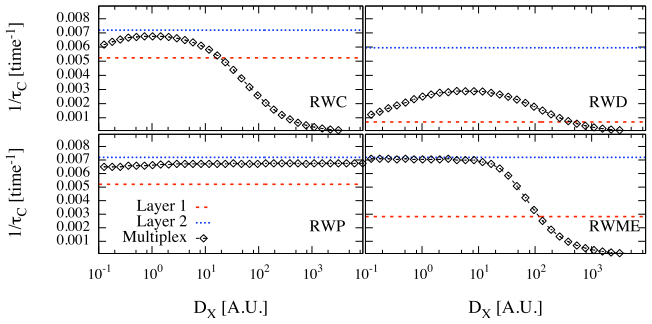

Fig. 5. Critical dependence of the coverage on navigation strategy and inter-layer connection strength. Different random walks are used to calculate the inverse of the time τ_C required to cover the 50% of a BA+ER multiplex with 200 vertices, as a function of $D_X = D^{12} = D^{21}$. The values for walks in each layer are shown for comparison and make clear how different exploration strategies have a strong effect on the coverage time scale.

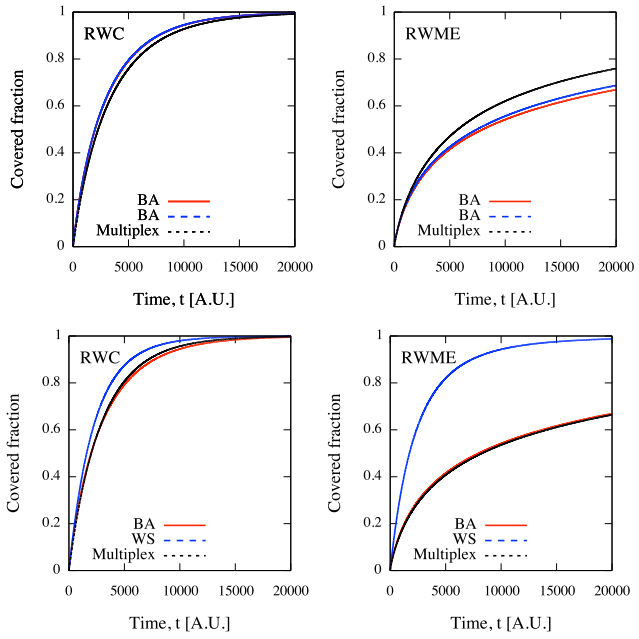

Fig. 6. Different types of diffusion characterize different topological structures and navigation strategies. Coverage *versus* time for two different multiplex topologies (BA+BA on the top panels and BA+WS on the bottom panels) and two different walk rules (RWC on the left panels and RWME on the right panels). While the diffusion on single layers separately and on the multiplex is similar for RWC on BA+BA, this is not the case for RWME on BA+BA where enhanced diffusion is shown in the multiplex. In the other cases, the diffusion is *infra*-diffusive.

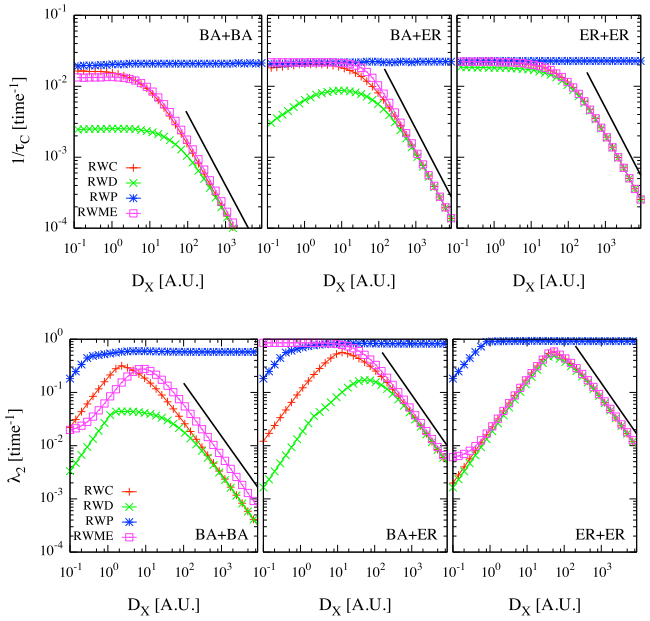

Fig. 7. Relation between dynamical and topological descriptors of a multiplex. Inverse of the time required to cover 50% of the network (top panels) and second smallest eigenvalue of the supra-Laplacian (bottom panels) as a function of D_X for three different multiplex topologies and different random walk. The solid straight line indicates D_X^{-1}. These results show an intimate relationships between the structure of the multiplex and the dynamics of the stochastic process taking place on it.

$\mathcal{C}_{r,s}(1)$ the smallest among all such constants. In the worst case, all terms equally contribute to $\rho(\tau^\star)$ and, therefore, the following inequality is satisfied:

$$\rho^\star \leq 1 - e^{-\mathcal{C}_{r,s}(1)\tau^\star - \mathcal{C}_{r,s}(2)\lambda_2^{-1}}. \qquad [7]$$

A rough estimation τ of $\tau^\star$ can be obtained by always considering the case with equality in the above formula, leading to

$$\tau \approx -\frac{\frac{\mathcal{C}_{r,s}(2)}{\lambda_2} + \log(1-\rho^\star)}{\mathcal{C}_{r,s}(1)}. \qquad [8]$$

By using the Perron-Frobenius it is possible to show that $\mathcal{C}_{r,s}(1) \geq 0$. To have a positive value of τ, the numerator in Eq. (8) should be negative, i.e., we are able to provide an estimation only for temporal scales such that the corresponding coverage satisfies the additional constraint $\rho^\star > 1 - \exp\left[-\mathcal{C}_{r,s}(2)\lambda_2^{-1}\right]$.

From Eq. (8) it is evident the strong influence of λ_2 on the inverse coverage time. The constants $\mathcal{C}_{r,s}(1)$, playing a crucial role in the time evolution of the coverage, explicitly depend on eigenvector centralities and are smaller for more peripheral vertices which are less reachable because of the topological structure and the nature of the walk.

It is also worth investigating the behavior of Eq. (6) in the limit of small or large values of D_X, i.e., the inter-layer strength and, in the following, we focus on classical and diffusive random walks.

In [10] it has been shown that in the limit $D_X \longrightarrow \infty$ there are eigenvalues converging to a constant value and other eigenvalues diverging proportionally to D_X. The eigenvalues obtained from the normalized supra-Laplacian in the case of random walkers are related to the eigenvalues of the diffusion process by $\lambda_\ell \propto \lambda_\ell^{\mathrm{Diff}}/D_X$. Substituting $\lambda_2 \propto D_X^{-1}$ in Eq. (6) we obtain that the time required to cover any given fraction of the multiplex is larger for increasing values of D_X. Our numerical experiments verify this theoretical expectation. An intuitive explanation is that when D_X is much larger than the average vertex strength, the random walkers spend most of the time in switching layer instead of jumping to other vertices. In the specific case of RWP each switching action is followed by a jump within the same time step and, therefore, for this type of walk the time to cover a given fraction of the multiplex is not influenced by D_X.

With a similar argument and the results obtained in [10], we have $\lambda_2 \propto D_X$ when $D_X \longrightarrow 0$. This extremal case corresponds to a multiplex with vanishing inter-layer connections and the resulting coverage is no more dependent on the value of D_X, reducing Eq. (6) to the coverage for a single layer.

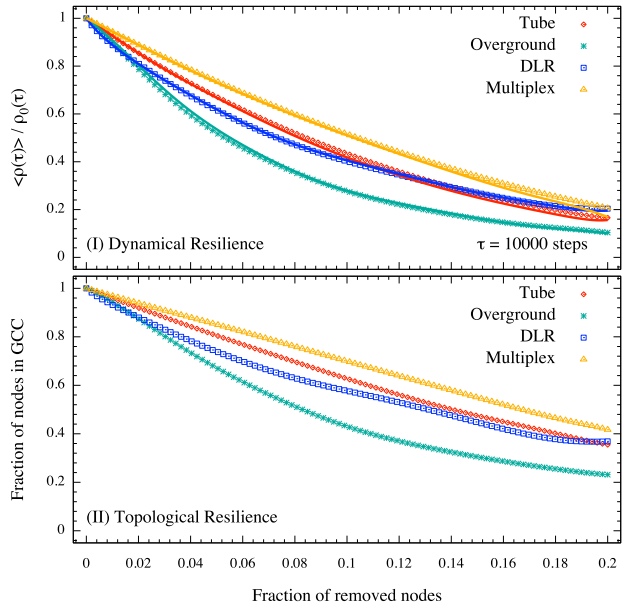

Fig. 8. Resilience of the public transport network of London to random failures. I) Theoretical expectations (solid lines) reproduce with great accuracy the resilience (points) obtained from simulations for each transportation layer and the whole interconnected system ($D_X = 10^{-1}$), assuming random-walk based navigation. II) Structural resilience, defined as the average fraction of vertices surviving in the giant connected component after random failures.

Dynamical vs Topological Resilience

We capitalize on the presented theoretical framework to investigate the navigability resilience of interconnected networks to random failures, focusing on the particular case of the public transport of London. A failure, here, is considered as the inoperability of a station in a certain transportation layer (e.g. because of an accident, a traffic jam, or catastrophe). Such an event can happen randomly on the system and can affect one or more stations at the same time. A measure of the operability of the full system in response to unexpected failures, can be inferred from the coverage of the respective networks after such events. This is what we call the *navigability resilience*. The resilience $r(\phi)$ of the system to a fraction ϕ of random failures is defined by $r(\phi) = \langle \rho_\phi(\tau) \rangle / \rho_0(\tau)$, where $\rho_\phi(t)$ is the coverage at time τ of the network subjected to ϕ failures and the averages are calculated over several random realizations of the failures. The normalization guarantees a fair comparison between the resilience of the multiplex and the monoplex networks. When a vertex fails in a single transportation layer, it can not be traversed by any path. However, if that vertex is part of an interconnected network it can be still reached on other layers. This intrinsic feature of multiplexes enhances the resilience of the system with respect to monoplexes, as shown in Fig. 8-I for the public transport of London.

We show in Fig. 8-II the topological resilience corresponding to the same multiplex, defined by the average fraction of vertices surviving in the giant connected component after random failures. The navigability, i.e. the dynamical resilience, is inherently smaller than the topological resilience of this multiplex network.

Empirical data of real disrupted services in London

Finding information about possible disruptions in the transportation network of London, from the Oyster data in our possession (see the Main text for information), is not trivial. Moreover, it is difficult to collect information about disruptions occurring in 2009, the period in which our Oyster data refers to. For this reason, we have opted for collecting new data about disrupted services in London during a more recent period of time.

Our first choice has been the official data provided by Transport for London (TfL). Such data is provided in real time but, unfortunately, it concerns only "Tube departure boards, line status and station status", with no support for disruptions occurring to Overground and DLR, two out of three layers in the multiplex transportation network considered in this study. Moreover, it is not possible to access to historical disruptions.

For this reason, we decided to gather data from Twitter. In fact, delays and disruptions are reported in real time in this online social network by means of many different accounts, each one corresponding to a particular line. For our data collection, we considered tweets sent by the following accounts: TfLTravelAlerts, bakerlooline, metline, wlooandcityline, circleline, victorialine, LDNOverground, jubileeline, districtline, northernline, hamandcityline, LondonDLR and piccadillyline. We collected all the tweets containing the string "no service" in the message, sent from those accounts between 11 February 2012 and 26 March 2014. The two years of data guarantees a fair representation of the true distribution of disrupted services. Our choice is justified by the fact that we consider disrupted stations, not delays in the traffic. We collected more than 3000 tweets and, by means of conservative heuristics, we classified 64% of them into 357 unique pairs of disrupted stations.

Here, we report some representative examples of the latest tweets in our dataset, together with information about the account who sent the tweets and the date. Many tweets are just reply to other users:

```
Account:   LDNOverground
Date:   15 mar 2014
Message:
@alexandrafinlay there's no service on that line
today. i advise you to de-select london overground
from the search. i'll pass this on too
```

Such tweets are not used to classify disruptions. The rest of the tweets do not use a standard format and heuristics have been used to parse the information, conservatively. For instance, messages like

```
Account:   LDNOverground
Date:   9 mar 2014
Message:   no service between richmond - camden road,
shepherds bush- willesden junction & watford junction-
queens park due to planned  upgrade work.
```

are difficult to be parsed, because the usage of symbols "&" and "-" is somehow arbitrary. Nevertheless, our algorithm is able to recognize at least the disrupted pair "richmond / camden road". Apart from this type of tweets with ambiguous syntax, the majority of them have been correctly parsed. For instance, the algorithm correctly finds the multiple disrupted pairs "euston / harrow&wealdstone", "harrow&wealdstone / watford" in

```
Account:   LDNOverground
Date:   14 set 2014
```

Table 2. Real disruptions in London transportation network, ranked by their occurrence in our dataset. The partially disrupted line ("Line" column) is reported, together with the starting ("From" column) and ending ("To" column) stations affected by the disruption. The rate of occurrence ("Freq." column) is also reported together with the fraction of stations indirectly affected ("Affected" column).

ID	Line	From	To	Freq.	Affected
DISR1	metropolitan	aldgate	bakerstreet	3.35%	2.44%
DISR4	overground	claphamjunction	surreyquays	2.02%	1.90%
DISR3	dlr	beckton	canningtown	2.56%	2.44%
DISR2	hammersmith&city	barking	moorgate	2.89%	3.52%
DISR9	piccadilly	raynerslane	uxbridge	1.53%	1.90%
DISR8	overground	claphamjunction	willesdenjunction	1.57%	1.63%
DISR7	piccadilly	actontown	uxbridge	1.57%	4.07%
DISR6	northern	edgware	hampstead	1.82%	1.90%
DISR5	overground	richmond	willesdenjunction	1.94%	1.63%
DISR26	metropolitan	aldgate	wembleypark	1.07%	2.98%
DISR25	overground	richmond	stratford	1.07%	6.23%
DISR24	metropolitan	aldgate	harrow-on-the-hill	1.12%	3.79%
DISR23	district	ealingbroadway	turnhamgreen	1.11%	1.36%
DISR22	overground	highbury&islington	newcross	1.11%	3.52%
DISR21	overground	camdenroad	richmond	1.16%	4.07%
DISR20	northern	camdentown	kennington	1.16%	2.71%
DISR19	metropolitan	northwood	wembleypark	1.16%	2.17%
DISR18	dlr	bowchurch	stratford	1.20%	0.81%
DISR17	overground	sydenham	westcroydon	1.24%	1.36%
DISR16	northern	camdentown	millhilleast	1.28%	2.17%

```
Message:   (1 of 2) no service btn euston - harrow &
wealdstone and severe delays btn harrow &
wealdstone - watford junction.
```

or "bank / poplar", "bank / west india quay", "tower gateway / poplar" and "tower gateway / west india quay"

```
Account:   LondonDLR
Date:   21 set 2014
Message:   morning, ahmed & alex providing updates.
due to planned work there is no service today between
bank/tower gateway and poplar/west india quay
```

or "bank / canning town", "tower gateway / canning town" and "stratford / canary wharf" in

```
Account:   LondonDLR
Date:   23 mar 2014
Message:   no service btn bank / tower gateway and
canning town / canary wharf, and also between
stratford and canary wharf. replacement buses operate.
```

where "btn" and "between" are used for the same purpose. It is worth remarking here that this dataset is not intended to provide us with complete information about real disruptions occurring in London, but only to provide a fair sample of reasonable and most frequent disruptions, to be used as input in our simulations.

The information about disruptions occurring to whole lines has been extracted manually from the data, without the usage of heuristics. However, for sake of completeness, we found reasonable to test all possible full-line disruptions (for a total of 11 possible disrupted multiplexes, excluding Overground and DLR which in our case are considered layers by themselves).

Here, we report details about some disruptions, ordered by their rank with respect to specific criteria. For instance, we consider:

- **Disruptions ranked by their frequency**. Here, frequency is calculated with respect to the data we have collected, and this is only a proxy for the true frequency of each disruption. Moreover, the most frequent disruptions are not, in general, the most dangerous for the traffic, involving only a limited amount of affected stations and often guaranteeing the connectedness of the underlying network. See Tab. 2.

- **Disruptions ranked by the number of stations they affect**. Here, disruptions might be more critical for the navigability of the system with respect to the previous ones. See Tab. 3.

- **Whole-line disruptions**. Disruption of a complete tube line is considered in each scenario, for a total of 11 lines. See Tab. 5.

In Tab. 4 we report the dynamical resilience calculated, numerically and theoretically, for some representative real partial disruptions, mainly sampled from Tab. 2 and Tab. 3. In Tab. 5 we report the same analysis for disruptions of whole lines. The values of the data-driven simulations are in remarkable agreement with our theory.

Table 3. Real disruptions in London transportation network, ranked by the number of stations they affect. The partially disrupted line ("Line" column) is reported, together with the starting ("From" column) and ending ("To" column) stations affected by the disruption. The rate of occurrence ("Freq." column) is also reported together with the fraction of stations indirectly affected ("Affected" column).

ID	Line	From	To	Freq.	Affected
DISR325	northern	eastfinchley	morden	0.04%	7.05%
DISR281	northern	goldersgreen	morden	0.04%	6.78%
DISR25	overground	richmond	stratford	1.07%	6.23%
DISR245	piccadilly	actontown	arnosgrove	0.04%	6.78%
DISR88	northern	edgware	kennington	0.33%	5.15%
DISR61	overground	claphamjunction	stratford	0.45%	5.96%
DISR44	overground	highbury&islington	westcroydon	0.58%	5.69%
DISR347	district	earlscourt	westham	0.04%	5.69%
DISR322	overground	southacton	stratford	0.04%	5.42%
DISR250	jubilee	stratford	willesdengreen	0.04%	5.42%
DISR227	metropolitan	aldgate	rickmansworth	0.08%	5.42%
DISR220	overground	hackneywick	richmond	0.08%	5.96%
DISR199	metropolitan	aldgate	croxley	0.08%	5.42%
DISR195	district	towerhill	upminster	0.08%	5.42%
DISR184	northern	millhilleast	stockwell	0.08%	5.15%
DISR181	northern	highbarnet	stockwell	0.08%	5.96%
DISR180	metropolitan	aldgate	uxbridge	0.08%	5.96%
DISR175	hammersmith&city	bakerstreet	barking	0.12%	5.15%
DISR151	district	embankment	upney	0.12%	5.15%
DISR140	northern	highbarnet	kennington	0.17%	5.42%

Table 4. Real partial disruptions in the London transportation network. Representative disruptions are considered, together with the starting ("From" column) and ending ("To" column) stations affected by the disruption. The rate of occurrence ("Freq." column) is reported, together with the fraction of stations indirectly affected ("Affected" column). It is indicated if the resulting multiplex is disconnected in 2 or more components ("Discon.?" column). The resilience obtained from Monte Carlo simulations (random walk and shortest-path based) are reported together with our theoretical expectation.

ID	Line	From	To	Freq.	Affected	Discon.?	Th.Res.	RW Res.	SP Res.
DISR1	metropolitan	aldgate	bakerstreet	3.35%	2.44%	NO	99.60%	100%	99.99%
DISR4	overground	claphamjunction	surreyquays	2.02%	1.90%	YES	92.34%	90.56%	100%
DISR3	dlr	beckton	canningtown	2.56%	2.44%	YES	94.41%	93.10%	94.85%
DISR325	northern	eastfinchley	morden	0.04%	7.05%	YES	85.90%	82.52%	87.07%
DISR25	overground	richmond	stratford	1.07%	6.23%	YES	89.07%	91.53%	97.90%
DISR245	piccadilly	actontown	arnosgrove	0.041%	6.78%	YES	88.50%	86.51%	90.85%
DISR181	northern	highbarnet	stockwell	0.083%	5.96%	YES	86.11%	82.55%	84.49%
DISR61	overground	claphamjunction	stratford	0.45%	5.96%	YES	86.59%	84.99%	99.66%
DISR119	northern	charingcross	highbarnet	0.25%	4.61%	YES	90.67%	87.99%	91.32%

Table 5. Complete line disruptions in London transportation network. Same as table 4, but also indicating if the resulting multiplex is disconnected in 2 or more components ("Discon.?" column). The resilience obtained from Monte Carlo simulations (random walk and shortest-path based) are reported together with our theoretical expectation.

ID	Line	Affected	Discon.?	Th.Res.	RW Res.	SP Res.
DISR-L1	bakerloo	6.78%	YES	95.80%	96.25%	99.79%
DISR-L2	circle	9.49%	NO	99.68%	100%	99.93%
DISR-L3	district	16.26%	YES	89.37%	89.47%	96.61%
DISR-L4	hammersmith&city	7.86%	YES	99.18%	99.460%	99.71%
DISR-L5	jubilee	7.32%	YES	91.50%	93.08%	100%
DISR-L6	metropolitan	9.21%	YES	91.96%	91.53%	95.43%
DISR-L7	northern	13.55%	YES	84.41%	80.98%	89.51%
DISR-L8	piccadilly	14.36%	YES	85.07%	83.43%	91.23%
DISR-L9	victoria	4.34%	YES	95.33%	96.78%	100%
DISR-L10	central	13.27%	YES	83.35%	80.49%	90.00%
DISR-L11	waterloo&city	0.54%	NO	99.98%	100%	100%

1. Stanley HE, Kang K, Redner S, Blumberg RL (1983) Novel superuniversal behavior of a random-walk model. *Phys. Rev. Lett.* 51:1223–1226.

2. Sinatra R, Gómez-Gardeñes J, Lambiotte R, Nicosia V, Latora V (2011) Maximal-entropy random walks in complex networks with limited information. *Phys. Rev. E* 83:030103.
3. Wilson RJ (1972) *Introduction to graph theory* (Academic Press New York) Vol. 111.
4. Tetali P (1991) Random walks and the effective resistance of networks. *J. Theor. Probab.* 4:101–109.
5. Noh JD, Rieger H (2004) Random walks on complex networks. *Phys. Rev. Lett.* 92:118701.
6. Yang SJ (2005) Exploring complex networks by walking on them. *Phys. Rev. E* 71:016107.
7. Samukhin A, Dorogovtsev S, Mendes J (2008) Laplacian spectra of, and random walks on, complex networks: Are scale-free architectures really important? *Phys. Rev. E* 77:036115.
8. Burda Z, Duda J, Luck J, Waclaw B (2009) Localization of the maximal entropy random walk. *Phys. Rev. Lett.* 102:160602.
9. Watts D, Strogatz S (1998) Collective dynamics of "small-world" networks. *Nature* 393:440–442.
10. Gómez S, et al. (2013) Diffusion dynamics on multiplex networks. *Phys. Rev. Lett.* 110:028701.